Biointerface Research in Applied Chemistry
Open-Access Journal (ISSN: 2069-5837)

Article
Volume 13, Issue 5, 2023, 432
https://doi.org/10.33263/BRIAC135.432

New Quantum Approach on Epilepsy Drug 3'-Aminothymidin Based on Pharmacokinetic, Topological and Molecular Docking Report

Herri Trilaksana [1], Thanmayalaxmi Darbhe [2], Athisaya Raja Suvitha [3,*], Rajesh Gangatharan [6], Anjali Nayak [4], Paramita Das [5]

1 Department of Physics, Faculty of Science and Technology, Airlangga University, Surabaya 60115, Indonesia; herri-t@fst.unair.ac.id (H.T.);
2 Department of Physics, CMR Institute of Technology (VTU), Bangalore, Karnataka, India; thanmayalaxmid@gmail.com (T.D.);
3 Department of Physics, CMR Institute of Technology, Bangalore, Karnataka, India; suvidanam@gmail.com (A.S.);
4 Department of SOD, CMR University, Bagalur, Bangalore, Karnataka, India; rajesh.visualart@gmail.com (A.N.);
5 Department of Pharmaceutical Chemistry, Krupanidhi College of Pharmacy, Bengaluru, Karnataka. 560035; anjaliangle84@gmail.com (P.D.);
6 Department of Pharmaceutical Chemistry, Krupanidhi College of Pharmacy, Bengaluru, Karnataka. 560035; paramitadas04@gmail.com (R.G.);
* Correspondence: suvidanam@gmail.com (A.S.);

Scopus Author ID 57218331018
Received: 1.07.2022; Accepted: 30.07.2022; Published: 16.12.2022

Abstract: In recent years, agricultural development has been one of the most significant initiatives. When introducing a product, it is essential to take into account clinical testing using ADMET qualities, pharmacokinetic properties, topological area, mass spectral analysis, and a report on microspecies dispersion. The creation of in silico models has been hampered by the desire of bio researchers. Pharmacokinetic properties control the amount of agricultural products consumed and how the body handles drugs. The current DFT research will help the biological industry adopt a new strategy for drug development. We investigated various aspects of the drug azidothymidine (AZDM). A variety of useful azidothymidine production values were discovered after further research into the docking results against two protein targets of the SNX2 gene for their antiepileptic activity.

Keywords: AZDM, ADMET, topological polar surface area, pharmacokinetic properties, Health care drug development

1. Introduction

In the fields of medicinal chemistry and drug development, increasing efficiency has taken on increasing importance. When operating at the quantum mechanical level, studying biological systems necessitates choosing a method that can yield substantial data in a constrained amount of time. Very little research has been done on the ecotoxicology of pharmaceuticals in environments. According to the fundamental tenet of logical drug design, the drug effect is produced by molecular recognition followed by the binding of a ligand to the active site of a target molecule. Therefore, determining the structure and strength of the binding interaction between the drug molecule and its target plays a crucial role in the drug design process. DFT is used frequently in the literature to examine potential drug-target interactions, demonstrating its suitability for drug property studies [1–4]. The current work aids in

comprehending the AZDM's various properties and bioactivity. The topological and ADMET properties are also calculated, and conclusions are drawn from them.

Calculations and studies are done on the topological and ADMET properties of the AZDM. Topological polar surface area (TPSA) has grown to be a very important topic, and its initial report has become very well-liked for virtual drug screening [5-8]. The same property is very helpful in predicting ADMET properties and Blood-Brain Barrier tendency, according to our literature review [9–18]. It is possible to study and create new biomolecules using mass spectrometry. The drug's topological surface area is predicted by the amount of molecular surface area produced by the polar atoms nitrogen, oxygen, and their attached hydrogen atoms. Understanding how drugs interact with organisms is made much easier by understanding their pharmacokinetic properties. How a drug interacts with a target macromolecule's binding sites determines its suitability. The drug's topological surface area predicts the molecular surface area arising from the polar atoms, which include nitrogen, oxygen, and their linked hydrogen atoms. The values of the corresponding properties have been tabulated, and the aforementioned properties have been calculated. The proposed use of AZDM as a key drug in organic farming is thus based on the present work's focus on various concepts in product production. As efficient techniques for accelerating the spread, variety generation, and quality improvement of medicine, molecular studies have come to the fore. The present study offers useful applications for the field of drug design, and several of these are currently in use. The scope and applicability of DFT in the research of drug-like molecules and their properties are briefly discussed in this review.

2. Materials and Methods

For the studies, AZDM of spectroscopic grade is bought and studied. A Marvin sketch is created to comprehend the structure of chemical bonds and functional groups. In order to advance drug development, Swiss ADME is used to analyze the characteristics of ADMEs, pharmacokinetics, drug-like existence, and limited molecular medicinal chemistry.

2.1. Protein preparation.

The gene for SNX27 (sorting Nexin 27), which encodes for proteins like 4HAS and 7PCB, was found in the RCSB PDB. The protein data bank's proteins were downloaded in PDB format. In MOE 2018, the proteins underwent energy minimization and removed water, ions, and ligand. Polar hydrogens, Kollman, and gasteiger charges were added using AutoDock 4.2 to prepare the target in PDBQT format.

2.2. Ligand preparation.

For the study against epilepsy, PubChem provided the ligand in 3D form. It was obtained in SDF format, and Open Babel software was used to convert it to PDB format. Torsion settings for the ligand are made using AutoDock 4.2 and saved in PDBQT format for docking studies.

3. Results and Discussion

3.1. Mass spectroscopy studies.

Mass spectrometry is now applied to research and create new molecular structures in the industry and other relevant fields. Mass spectrometry is a destructive method for estimating molecular weight and getting molecular structural information. The material is ionized and not subjected to electromagnetic radiation, which sets it apart from previous techniques. When ionized chemicals are stimulated, fragmentation occurs. From studying such fragments, the arrangement of molecules can be determined. Each fragment's mass-to-charge ratio, or m/z, specifies its identity, and devices can differentiate and detect such ions. The mass differences between molecular ions and fragments must match a real chemical composition. Bond fragmentation is influenced by several aspects, including bond strength, the likelihood of a low-energy transition, and the stability of emerging pieces.

Figure 1 shows the fragmentation and product ion spectra produced by injecting AZDM analytical standards directly. The mass/charge ratio (m/z) values of AZDM and the electrospray ionization fragments were then used to quantify the compound in the samples. Fig 1 displays the potential MS/MS collisional induced dissociation (CID) methods for AZDM (m/z: relative abundance are 267: 1.00 268: 0.13 269: 0.02) due to a lack of information surrounding the atoms' fragmentation. The chemical composition of AZDM is C (44.94%), H (4.90%), N (26.21%), O (23.95%). The m/z values discovered in this study are consistent with previous findings in samples containing anthocyanidins [19-21]. All the compounds were finally identified with increased laser power and an ion gate tuned to the corresponding masses. The breaking of a glycosidic link, shown to be universal to all anthocyanin derivatives, causes the peak. Because the core of an anthocyanin molecule can be recognized, fragment monitoring makes identifying this class of substances much easier.

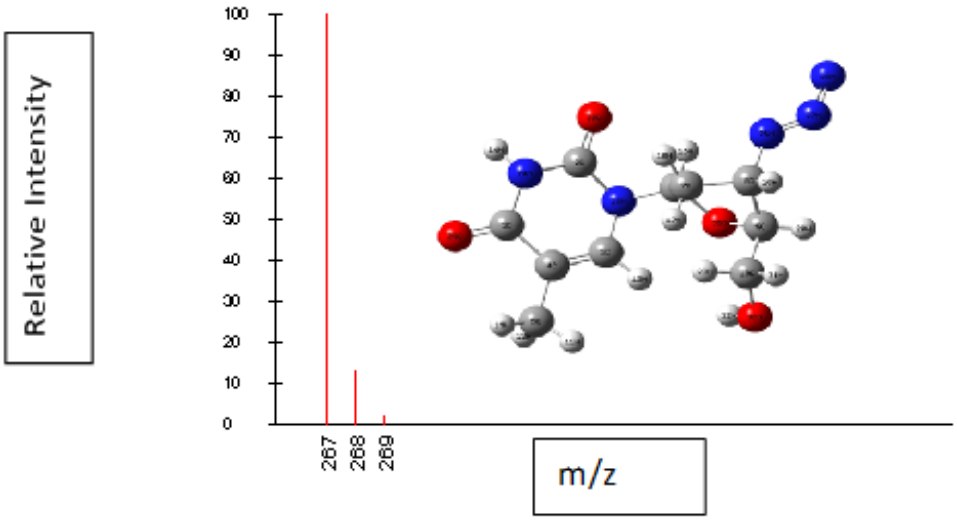

Figure 1. Mass Spectrum of AZDM.

3.2 Topological and ADMET properties.

The physical compound and ADMET property counts were completed using the ADMET indicator instrument [22] and the Swiss ADMET programming recreation [23]. ADMET Predictor is a productivity tool that quickly and accurately predicts over 40 properties, such as dissolvability, logP, CYP digestion positions, and Ames mutagenicity. Bioactivity

radar is being studied in terms of six physicochemical characteristics. The pink site discusses where each function should be held. The logP of a particle requires the extension of its molecules. Bioavailability radar can be used to measure a molecule's drug-likeness quickly. The ADMET Predictor has a simple user interface that conveniently tracks and calculates values for various compounds. Tables 1, 2, 3, 4, 5, and 6 reveal that the ADMET (Absorption, Distribution, Metabolism, Excretion, and Toxicity) findings are useful descriptors, particularly for biological boundary-crossing such as brain access and absorption [24]. In Figure 2, the molecular structure has been indicated using a Vander Waals prediction.

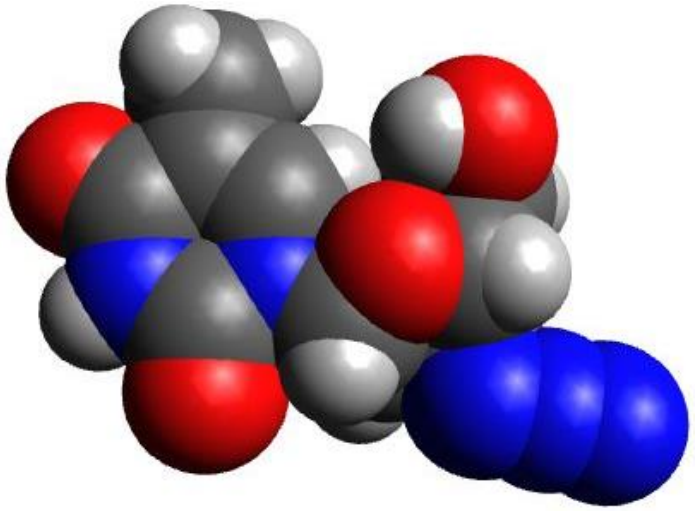

Figure. 2. Vander Waals prediction of AZDM.

The topological polar surface areas of the selected compounds are 97.99 Å², 57.53 Å², 269.43 Å², and 131.36 Å², respectively, indicating high intestinal absorption. Topological and structural descriptors are essential molecular descriptors for predicting bioactivity [25-27]. The physiochemical parameters are more responsible for receptor binding activity than topological parameters. The structure was drawn using the Marvin sketch 5.0 tool, and a 3D model was developed using the same program; topological descriptors were also determined.

Table 1. ABS of AZDM.

ABS	AZDM
WS (log mol/L)	-3.517
$CaCo_2$ PERM (log Papp in 10-6 cm/s)	-0.154
Int.ABS (human) (% Absorbed)	70.225
Skin Perm. (log Kp)	-3.142
P-glycoprotein subst.	No
P-glycoprotein I inhib.	No
P-glycoprotein II inhib.	No

ABS: Absorption, WS: Water Solubility, PERM: permeability, Int.ABS: Intestinal Absorption, Skin Perm.: Skin Permeability, Subs: substrate, inhib.: inhibitor.

Table 2. Distribution of AZDM.

Distribution	AZDM
VDss (hum.)(log L/kg)	0.036
FUb (human)(Fu)	0.755
BBB perm. (log BB)	-1.166
CNS perm.(logPs)	-3.236

VDss (hum.): VDss human, FUb: Fraction Unbound, BBB perm.: BBB permeability, CNS perm.: CNS permeability.

Table 3. Metabolism of AZDM.

TXCTY	AZDM
AMES . TXCTY	No
MTD (hum.) (log mg/kg/day)	0.656
hERG I inhib.	No
hERG II inhib.	No
ORA TXCTY (LD50) (mol/kg)	2.298
ORC TXCTY (LOAEL) (log mg/kg_bw/day)	2.014
HPTXT	Yes
Skin Sensitisation	No
T.Pyriformis TXCTY (log ug/L)	0.118
Minnow TXCTY (log mM)	3.145

Subs.: Substrate, Inhib.: Inhibitor.

Table 4. Excretion of AZDM.

Metabolism	AZDM
CYP2D6 subs.	No
CYP3A4 subs.	No
CYP1A2 inhib.	No
CYP2C19 inhib.	No
CYP2C9 inhib.	No
CYP2D6 inhib.	No
CYP3A4 inhib.	No

TL CL: Total Clearance, RL subs.: Renal Substrate.

Table 5. TXCTY of AZDM.

Excretion	AZDM
TL CL (log ml/min/kg)	0.052
RL OCT2 subs.	No
Metabolism	AZDM
CYP2D6 subs.	No
CYP3A4 subs.	No
CYP1A2 inhib.	No
CYP2C19 inhib.	No
CYP2C9 inhib.	No
CYP2D6 inhib.	No
CYP3A4 inhib.	No

TXCTY: Toxicity, MTD(hum.): Maximum Tolerated Dose (human), inhib.: Inhibitor, HPTXT: Hepatotoxicity, ORA: Oral Rat Acute, ORC: Oral Rat Chronic.

Table 6. Bioactive properties of AZDM.

Other Bioactive calculations	AZDM
GPCR ligand	0.41
ICM	-0.08
Kinase inhib.	-0.15
NRL	-0.79
Protease inhib.	-0.02
Enzyme inhib.	1.17

ICM: Ion Channel Modulator, inhib.: Inhibitor, NRL: Nuclear receptor ligand.

3.3. Structural analysis.

Ionic and covalent bond strengths are frequently investigated using DFT [28-30]. DFT is extremely accurate at predicting the strength of hydrogen bonds. The AZDM geometrical specifications of bond length (A^0) and bond angles (^{0}) were received by DFT in the B3LYP

technique with 6-311++G (d, p) base sets. The correlation graphs for the bond length and bond angle for AZDM are presented in Fig.3 & 4. In AZDM, the length of the bond of C9-031 within the tetrahydrofuran ring is 1.47A^o in DFT. The above value is well in line with the published figure of 1.45A^o reported with similar derivatives. The dihedral angles in tetrahydrofuran calculated using B3LYP/DFT methods are matched with the reported data [31-35]. C6-O31-C9 has a bond angle of 104^o, which is almost near 109.5^o [36]. Correspondingly, the bond length 1.23A^o of N26-N27 and N27-N28 is exactly in agreement with the values obtained from the literature [37]. The bond lengths and bond angle in the pyrimidine group calculated using B3LYP are in good relation with the literature values [38-40]. It is clear that geometrical analysis is growing to be very well-liked in the field of drug design research. Therefore, it is crucial to determine whether the structural bond length and angle are appropriate to describe properties important to study drugs.

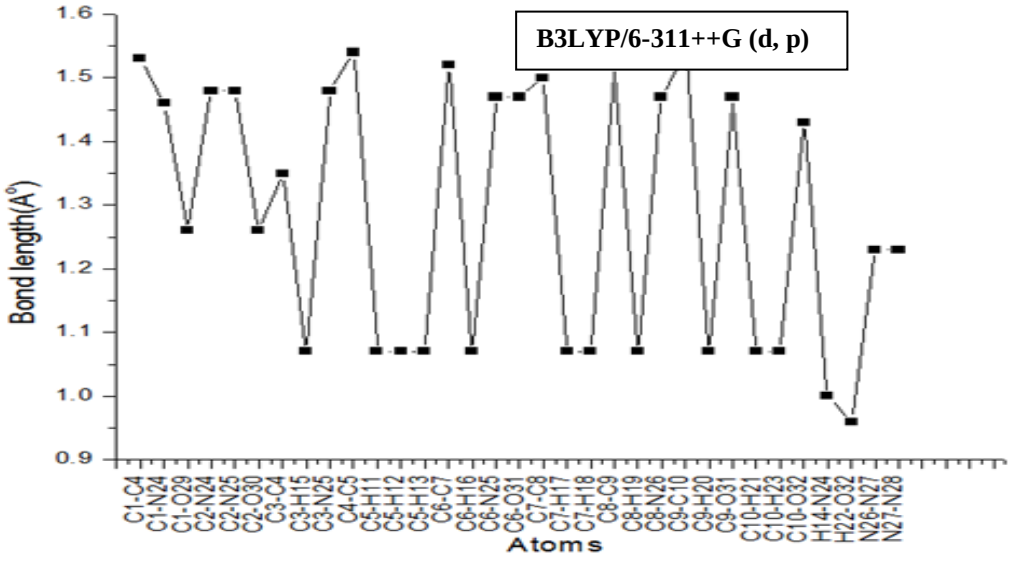

Figure 3. The bond length graph by B3LYP method on AZDM.

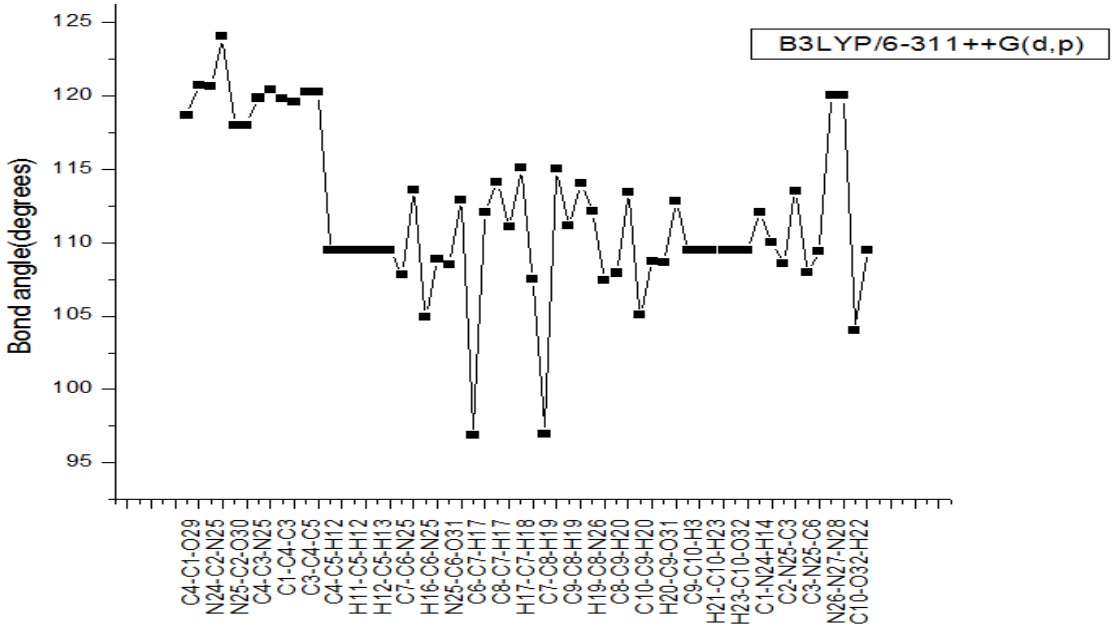

Figure 4. The graph for bond angles by B3LYP method on AZDM.

3.4. Biological activity and physicochemical parameters.

To compute physicochemical descriptors, Swiss ADME was used. It is a model to calculate and express ADME (absorption, distribution, metabolism, and excretion) parameters, a study of an organism affecting a drug (pharmacokinetic properties), drug nature, and therapeutic chemical reliability of small molecule AZDM, which were analyzed in Table 7. The remarkable biological activity of this compound may be arising from 1H-pyrimidine-2, 4-dione ring, and tetrahydrofuran, which play a remarkable role in antimicrobial activity. Bioavailability Radar is displayed for a quick evaluation of the molecule's drug-likeness. Six physicochemical properties are studied under AZDM. Adapted descriptors have established a physicochemical range on each axis. The pink site outlines the best possible area for each location. Figure 5 shows the optimized structure, Molecular lipophilicity ability, and Bioactivity radar on each axis, with adapted descriptors specifying a physicochemical range of the extracted compounds.

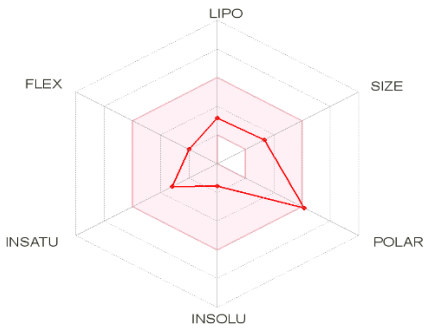

Figure 5. Physicochemical Bio radar representation of AZDM.

3.5. Pharmacokinetic properties and drug-like nature.

The compound's remarkable biological activity can result from 1H-pyrimidine-2, 4-dione ring, and tetrahydrofuran, which can play a major role in the antimicrobial function. The polar surface area of the molecule is 137.04A^2, which shows good intestinal absorption. This has proven a useful descriptor in models to determine some ADMET properties, especially a concern with biological barrier crossing such as brain access and absorption. In pharmacokinetics, the present molecule is confirmed to have strong Gastrointestinal (GI) uptake. The blood-brain barrier (BBB) is a concept used to characterize the special properties of the central nervous system (CNS) of the microvasculature. A drug-like nature gives information about the qualitative estimation of specific physicochemical properties that make a molecule possible for an oral drug. The bioavailability of the molecule is 56%. The present compound has BBB nil, which indicates that they represent highly hydrophilic, polar chemicals to predict intestinal permeation.

3.6. Micro species distribution.

The pH standard logarithm for the four microspecies of the AZDM, which are present in the range of 0 to 14, have been identified, as shown in figure 6. The functional groups of the protein can exist in a variety of protonation states that can be affected by ligands, with the promoter being the most stable within the binding site. Positively charged active sites provide a higher local pH, while negatively charged active sites provide a lower local pH.

Table 7. Biological activity and physicochemical parameters of AZDM.
Form: Formula, Mol.weight: Molecular weight, Num: Number, Solub.: Solubility, Abs.: Absorption, Inhib.: Inhibitors, Bio.av.score: Bioavailability score, Dr.likeness: Druglikeness, PK: Pharmacokinetics, accpt: acceptor, rot.: rotatable, Fract.: Fraction.

Physicochemical Properties		**Lipophilicity**	**distribution coefficients**
Form.	$C_{10}H_{13}N_5O_4$	Log_Po/w_(iLOGP)	1.93
Mol. weight	267.24 g/mol	Log_Po/w_(XLOGP3)	0.05
Num. heavy atoms	19	Log_Po/w_(WLOGP)	-0.52
Fract. Csp3	0.60	Log_Po/w_(MLOGP)	-1.25
Num. rot. bonds	3	Class	Soluble
Num. H-bond accpt.	7	Log_S_(SILICOS-IT)	-1.16
Num. H-bond donors	2	Solub.	1.84e+01 mg/ml ; 6.87e-02 mol/l
TPSA	134.07 Å²	Class	2
PK		Medicinal Chemistry	
GI abs.	High	PAINS	1 alert: azo_A
BBB permeant	No	Brenk	3 alerts: azido_group,diazo_group, quaternary_nitrogen_3
P-gp substrate	No	Lead like ness	Yes
CYP1A2 inhib.	No	Synthetic accessibility	3.93
CYP2C19 inhib.	No	Water Solubility	
CYP2C9 inhib.	No	Log_S_(ESOL)	-1.56
CYP2D6 inhib.	No	Solub.	7.29e+00 mg/ml ; 2.73e-02 mol/l
CYP3A4 inhib.	No	Class	Very soluble
Dr.likeness	Yes	Log_S_(Ali)	-2.42
Lipinski	No; 1 violation	Solub.	1.02e+00 mg/ml ; 3.81e-03 mol/l
Ghose	Yes	Log_S_(SILICOS-IT)	-1.16
Veber	No; 1 violation	Solub.	1.84e+01 mg/ml ; 6.87e-02 mol/l
Egan	Yes		
Muegge	0.56		
Bio.av. Score	Yes		

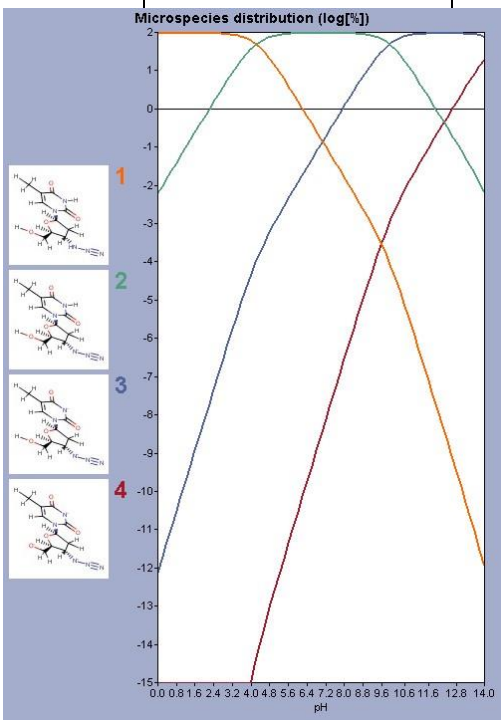

Figure. 6. Micro species distribution of AZDM.

As several functional groups undergo ionization at physical pH conditions, ionic interactions play a significant part in the mechanism of action of drugs. Unionized molecules may have dipole moments and can interact with other ions or dipoles to form ion-dipole or dipole-dipole bonds. Despite being less powerful than ionic interactions, both of these interactions are crucial for drug-receptor binding. Hydrogen bonds, hydrophobic interactions, and charge transfer interactions are weak interactions between a drug and a receptor to help stabilize the drug-receptor complex. Microspecies distribution is useful for predicting dispersion interactions between hydrogen bonds to hydrophobic interactions [41,42].

3.7 Docking studies.

The obtained target and ligand were docked using AutoDock 4.2. A grid box of 60 points each in XYZ dimensions is set as the boundary around the ligand for the AutoGrid program for determining suitable amino acid residue. After the AutoDock program, the results were analyzed, and the interactions were visualized using Discovery Studio Visualizer. Drug designing also has a lot of interest in the docking characteristics of drug molecules. It is possible to effectively study ionization energies, relative energies, electron affinities, and metal-ligand bond strengths. It shows a good binding affinity for target protein 7PCB as well as multipoint receptor interaction with major amino acids for binding as TYR448, ASN177, GLN79, GLY59, ARG58, LEU78, GLN60, PRO77, GLU63, ALA112. The characteristics of drug molecules and their interactions with their receptors are determined by their molecular structure. Therefore, the foundation of any computational drug study is the prediction of the docking analysis of the drug molecule.

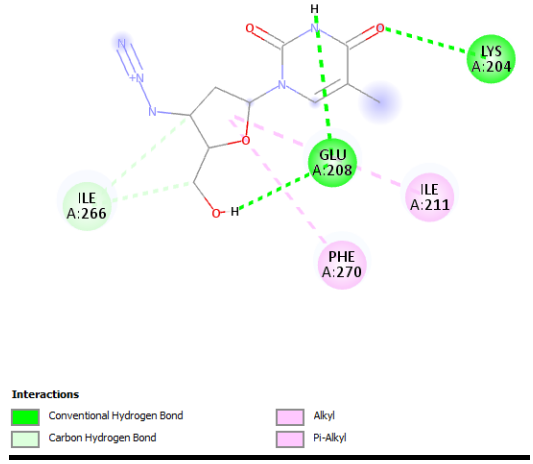

Figure 7. 2D interaction of Zidovudine with 4HAS.

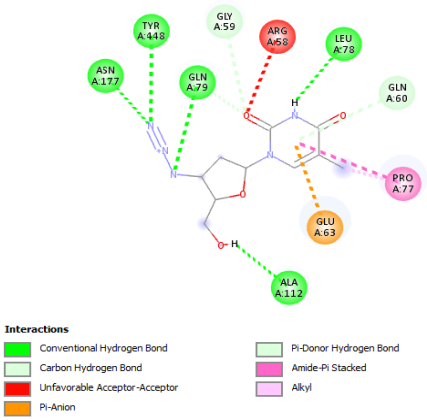

Figure 8. 2D interaction of Zidovudine with 7PCB.

4. Conclusions

AZDM has been investigated using a variety of parameters, and we discovered that it has some unique properties. Through this essay, we hope to draw attention to the significance of drug development in society. We have a unique opportunity to examine the structural and chemical properties of the molecule due to the various quantum chemical calculations. It improves immune performance and partially repairs HIV-related neurological damage. Additionally, it makes some clinical abnormalities linked to AIDS worse. These efficient descriptors and techniques can predict significant ADMET behavior of pharmacokinetics optimization and assessment of the current compound. The compound's topological surface area reveals that AZDM has a high intestinal absorption rate. Both the physicochemical parameters and a 3D model have been examined. The antiepileptic activity of two protein targets of the SNX27 (sorting Nexin 27) gene was examined in docking studies downloaded from PDB databases (PDB ID: 4HAS and 7PCB). The drug demonstrated binding affinity with respective scores of -6.65 and -6.94. The main amino acids for binding are TYR448, ASN177, GLN79, GLY59, ARG58, LEU78, GLN60, PRO77, GLU63, and ALA112. It exhibits good binding affinity for the target protein 7PCB and multipoint receptor interaction. Based on our analysis, biomedical scientists can use the aforementioned drug in combination with other proteins or other agents to accelerate drug development.

Funding

This research received no external funding.

Acknowledgments

We are thankful to the department of Physics, Faculty of Science and Technology, Airlangga University, Surabaya 60115, Indonesia, for computational software support.

Conflicts of Interest

The authors declare no conflict of interest.

References

1. Yohei K; Natalie H; Prediction of oral pharmacokinetics using a combination of in silico descriptors and in vitro ADME properties. *Mol. Pharm.* **2021**, 18, 1071-1079, https://doi.org/10.1021/acs.molpharmaceut.0c01009.
2. Sapse A M; Rothchild R; Lown J W; Semi-empirical, *ab Initio* and molecular modeling studies on the DNA binding of a calicheamicinone-polyamide conjugate. *J. Biomol Struct. Dyn.* **2000,** *18*, 423-431, https://doi.org/10.1080/07391102.2000.10506678.
3. De Esch I J; Timmerman H; Menge W M; Nederkoorn P H; A qualitative model for the histamine H3 receptor explaining agonistic and antagonistic activity simultaneously. *Arch Pharm* **2000,** *333*, 254-260, https://doi.org/10.1002/1521-4184(20008)333:8%3C254::aid-ardp254%3E3.0.co;2-g.
4. Mavri J; Hadži D; Modelling of ligand–receptor interactions: ab-initio and DFT calculations of solvent reaction field effects on methylated ammonium–π and–acetate complexes. *J.Mol.Struct. THEOCHEM* **2001**, *540*, 251-255, https://doi.org/10.1016/S0166-1280(00)00733-8.
5. DeSarno.; Alexandra E; Parcell, Benjamin J.; Coote, Peter J .; Repurposing the anti-viral drug zidovudine (AZT) in combination with meropenem as an effective treatment for infections with multi-drug resistant, carbapenemase-producing strains of Klebsiella pneumoniae. *Pathogens and Disease* **2020**, *78*, https://doi.org/10.1093/femspd/ftaa063.

6. Nouraliei, M.; Karimkhani, M.; Mansouri, S.; and Bagheri, Z.;Geometry-controlled carbon nanostructures as effective drug delivery carriers for MAO enzyme inhibitors: A DFT study. *J. Mol. Liq*. **2021**, *340*, 116857, https://doi.org/10.1016/j.molliq.2021.116857.
7. Mazumdar, P.; Choudhury, D.; and Borgohain, G.; A DFT and molecular dynamics simulation study of single-walled carbon nanotube as a drug delivery system for few model nitrogen mustard drugs. *J.Mol.Struct.* **2021**,*1243*, 130877, https://doi.org/10.1016/j.molstruc.2021.130877.
8. Monge A.; Arrault A.; Marot C.; Morin-Allory L.; Managing, profiling and analyzing a library of 2.6 million compounds gathered from 32 chemical providers. *Molecular Diversity* **2006**, *10*, 389–403, http://dx.doi.org/10.1007/s11030-006-9033-5.
9. Devi, R.N.; Stephen, A.D.; Justin, P.; Saravanan, K.; Macchi, P.; and Jelsch, C.; Topological and electrostatic properties of diclofenac molecule as a non-steroidal anti-inflammatory drug: An experimental and theoretical study. *J.Mol.Struct.* **2019,** *1196*, 42-43, https://doi.org/10.1016/j.molstruc.2019.06.027.
10. Jeelani, A.; Muthu, S.; Ramesh, P.; and Irfan, A.; Experimental spectroscopic, molecular structure, electronic solvation, biological prediction and topological analysis of 2, 4, 6-tri (propan-2-yl) benzenesulfonyl chloride: An antidepressant agent. *J.Mol.Liq.* **2022**, *358*, 119166, https://doi.org/10.1016/j.molliq.2022.119166.
11. Parakkal, S.C.; Datta, R.; Muthu, S.;Irfan, A.; and Jeelani, A.;. Computational investigation into structural, topological, electronic properties, and biological evaluation of spiro [1H-indole-3, 2′-3H-1, 3-benzothiazole]-2-one. *J.Mol.Liq.* **2022**, *359*, 119234, https://doi.org/10.1016/j.molliq.2022.119234.
12. Khezri, B.; Maskanati, M.; Ghanemnia, N.; Gokeh, M.S.; Rezaei, S.; and Chang, L.; Efficient detection of thioguanine drug using boron nitride nanocage: DFT outlook of solvent effect and AIM analysis. *In. Org. Chem. Comm.* **2021**, *134*, 109015, https://doi.org/10.1016/j.inoche.2021.109015.
13. Subrata D; Anthony A.R; Robert H; Rebecca B; ADME and pharmacokinetic properties of Remdesivir: Its drug interaction potential. *Pharmaceutics.* **2021**, 14(7), 655, https://doi.org/10.3390/ph14070655.
14. Suvitha, A.; El-Mansy, M.A.M.; Kothandan, G.; Steephen, A.; Molecular structure, FT-Raman, IR, NLO, NBO, HOMO–LUMO Analysis, Physicochemical descriptors, ADME Parameters, and pharmacokinetic bioactivity of 2, 3, 5, 6-Tetrachloro-p-benzoquinone *J. Struct. Chem*, **2021**. 62(9), 1339-1356, doi10.1134/S0022476621090031.
15. Madhavan, B.; Suvitha, A.; Steephen, A., Novel La1− xCaxTi1− yTayO3-δ perovskites with enhanced conductivity for solid oxide fuel cell electrodes. *J. Alloys Compd*. **2022**, 915, 165370, doi:10.1016/j.jallcom.2022.165370.
16. Yahya, M.; Kurtay, G.; Suvitha, A.R.; On the viability of divergent donor moieties in malononitrile-based donor-π-acceptor NLO active materials: A DFT/TD-DFT study. *J. Phys. Org Chem*. N **2022**, 35(10), e4403, https://doi.org/10.1002/poc.4403.
17. Seshan, G.; Kanagasabai, S. Ananthasri, S.; Kannappan, B.; Suvitha, A.; Jaimohan, S.M.;Kanagaraj, S.; Kothandan, G.; Insights of structure-based pharmacophore studies and inhibitor design against Gal3 receptor through molecular dynamics simulations. *J. Biomol. Struct. Dyn.*, **2021,** 39(18), 6987-6999.https://doi.org/10.1080/07391102.2020.1804452.
18. Yahya, M.; Suvitha, A; Bouziani, A.; Structural, photophysical and optoelectronic activity of triphenylamine-based push–pull chromophores: a theoretical study. Opt. Quant. Elect., **2022,** 54(12), 1-17. https://doi.org/ 10.1007/s11082-022-04239-w.
19. El-Mageed, H.A.; Mustafa, F.M.; and Abdel-Latif, M.K.; Boron nitride nanoclusters, nanoparticles and nanotubes as a drug carrier for isoniazid anti-tuberculosis drug, computational chemistry approaches. *J.Mol.Struct. Dynam.* **2022**, *40*, 226-235, https://doi.org/10.1080/07391102.2020.1814871.
20. Gerebtzoff, G.; and Seelig, A.; In silico prediction of blood− brain barrier permeation using the calculated molecular cross-sectional area as main parameter. *J. Chem. Inf. Model.* **2006**, *46*, 2638–2650, https://doi.org/10.1021/ci0600814.
21. Irfan, C.; Mehmet G; Halil G; Hidayet C; Yusuf S; Irfan K; Synthesis,dielectric properties, molecular docking and ADME studies of pyrrole-3-ones. *J. Biomol. Struct. Dyn.* **2021,** https://doi.org/10.1080/07391102.2021.1914174.
22. Zhang, Z.; Kou, X.; Fugal, K.; McLaughlin, J.; Comparison of HPLC Methods for Determination of Anthocyanins and Anthocyanidins in Bilberry Extracts. *J. Agric. Food Chem* **2004**, *52*, 688, https://doi.org/10.1021/jf034596w.
23. Abrankó, L.; Szilvássy, B.; Mass spectrometric profiling of flavonoid glycoconjugates possessing isomeric aglycones. *J. Mass Spectrum* **2015**, *50*, 71, https://doi.org/10.1002/jms.3474.

24. Pires, D.E.; Blundell, T.L.; and Ascher, D.B; pkCSM: predicting small-molecule pharmacokinetic and toxicity properties using graph-based signatures. *J. Med. Chem.* **2015**, *58*, 4066-4072, https://doi.org/10.1021/acs.jmedchem.5b00104.
25. Daina A.; Michielin O.; and Zoete V.; SwissADME: a free web tool to evaluate pharmacokinetics, drug-likeness and medicinal chemistry friendliness of small molecules. *Sci. Rep.* **2017**, *7*, 2717, https://doi.org/10.1038/srep42717.
26. Vivek, P.; Rekha, M.; Suvitha, A.; Kowsalya, M.; and Steephen, A. Diamond morphology CuO nanomaterial's elastic properties, ADMET, optical, structural studies, electrical conductivity and antibacterial activities analysis. *Inorg. Nano-Met. Chem.* **2022**, 1243-1255, https://doi.org/10.1080/24701556.2022.2046610.
27. Du, Q.; Mezey, P.G.; and Chou, K.C; Heuristic molecular lipophilicity potential (HMLP): A 2D-QSAR study to LADH of molecular family pyrazole and derivatives. *J.Comput.chem*. **2005**, *26*, 461-470, https://doi.org/10.1002/jcc.20174.
28. Jemmis E D; Giju K T; Leszcynski J E; Ionic to covalent bonding: a density functional theory study of linear and bent X2Y3 monomers (X=B, Al, Ga, In; Y=O, S, Se). *Electron J. Theor. Chem.* **2001**, *2*, 130-138, https://doi.org/10.1002/ejtc.37.
29. Mó O; Yáñez M; Eckert M M; Maksić Z B; Alkorta I; et al., Periodic trends in bond dissociation energies. A theoretical study. *J Physical Chem.* **2005**, *109*, 4359-4365, http://dx.doi.org/10.1021/jp050857o.
30. Allen EC; Beers K J, Ab initio study of the binding strength of POSS-cation complexes. *Polymer*. **2005**, *46*, 569-573, http://dx.doi.org/10.1016/j.polymer.2004.07.006.
31. Durgadevi, R.; Suvitha, A.; and Arumanayagam, T., Growth, optical, electrical properties and DFT studies on piperidinium 4-nitrophenolate NLO single crystal in acetone. *J.Cry. Growth*, **2022**, 582, 126512. https://doi.org/10.1016/j.jcrysgro.2021.126512.
32. El-Mansy, M.A.M.; Suvitha, A.; and Narayana, B., Exploring crystal, electronic, optical and NLO properties of ethyl 4-(3, 4-dimethoxy phenyl)-6-methyl-2-thioxo-1, 2, 3, 4-tetrahydro pyrimidine-5-carboxylate (MTTHPC). *Opt. Quan. Ele.* **2021**, *53*, 1-16, https://doi.org/10.1007/s11082-021-03057-w.
33. Durgadevi, R.; Suvitha, A.; Steephen, A.; and Arumanayagam, T., An organic hexamine p-nitrophenol crystal: Growth, optical, electrical, mechanical and density functional theoretical studies for nonlinear optical applications. *Opt. Mat.* **2022**, *127*, 112280, https://doi.org/10.1016/j.optmat.2022.112280.
34. El-Mansy, M.A.M.; Ibrahim, M.; Suvitha, A.; Abdelsalam, H.; and Osman, W. Boosted electronic, optical, and NLO responses of homo P-nanoclusters via conducting polymeric substituents. *Comp.Theo. Chem.* **2021**, *1202*, 113343, https://doi.org/10.1016/j.comptc.2021.113343.
35. Mohammadi, M.D.; Abdullah, H.Y.; and Suvitha, A., The adsorption of 1-chloro-1, 2, 2, 2-tetrafluoroethane onto the pristine, Al-, and Ga-doped boron nitride nanosheet. *Iran. J Sci. &Tech., Transactions A: Science* **2021**, *45*, 1287-1300, https://doi.org/10.1007/s40995-021-01117-0.
36. Ertl, P.; B. Rohde.; and P. Selzer.; Fast calculation of molecular polar surface area as a sum of fragment-based contributions and its application to the prediction of drug transport properties. *J. Med. Chem.* **2000**, *43*, 3714-3717, https://doi.org/10.1021/jm000942e.
37. Jones, P.G.;Kirby, A.J.; and Ryder, H., Bond length and reactivity. Structure of 2-(4-nitrophenoxy) tetrahydrofuran. Acta Crystallographica Section C: *Cry. Struc.Comm., Acta cryst*. **1989**, *45*, 239-241, http://dx.doi.org/10.1107/S010827018801128X.
38. V Furer, V.L.; Vandyukov, A.E.; Majoral, J.P.; Caminade, A.M.; Gottis, S.; Laurent, R.; and Kovalenko, V.I., Comparative DFT study of structure, reactivity and IR spectra of phosphorus-containing dendrons with PNPS linkages, vinyl and azide functional groups. *J. Mol. Stru.* **2015**, *1091*, 6-15, https://doi.org/10.1016/j.molstruc.2015.02.067.
39. Haritha, M.; and Suresh, C.H.; Hydration patterns of rings in drugs and relationship to lipophilicity: A DFT study. *J. Comp.Chem.* **2022**, *43*, 477-490, https://doi.org/10.1002/jcc.26808.
40. Anupama Sharma; Naveen Dhingra; Har Lal Singh; Sarita Khaturia; Uma Bharadwaj; New Complexes of organotin(IV) and organosilicon(IV) with 2-{(3,4-dimethoxybenzylidene)amino}-benzenethiol: Synthesis, spectral, theoretical, antibacterial, docking studies. *J. Mol.Struc*. **2022**, *1261*, 13281, https://doi.org/10.1016/j.molstruc.2022.132812.
41. Moradnia, H.; Raissi, H.; and Bakhtiari, A.; A density functional theory-based analysis of the structural, topological and electronic properties of gemcitabine drug adsorption on the pyrrolidine functionalized single-walled carbon nanotube. *J. Bio Mol. Struct. and Dyn.* **2019**, 2477-2486, https://doi.org/10.1080/07391102.2018.1491892.

42. Suvitha, A.; El-Mansy, M.A.M.; Kothandan, G.; Steephen, A. Molecular Structure, Ft-Raman, Ir, Nlo, Nbo, Homo–Lumo Analysis, Physicochemical Descriptors, Adme Parameters, And Pharmacokinetic Bioactivity Of 2, 3, 5, 6-Tetrachloro-P-Benzoquinone. *J. Struct. Chem.* **2021**, *62*, 1339-1356, https://doi.org/10.1134/S0022476621090031.